

Antibody-Based Methods Reveal the Protein Expression Properties of Glucosinolate Sulfatase 1 and 2 in *Plutella xylostella*

Yu Xiong,^{1,*} Chaoyang Jiang,^{2,*} Muhammad Bilal Amir,^{1,3,✉} Yuhong Dong,¹ Lianjie Xie,¹ Yuan Liao,¹ Weiyi He,^{4,5} Zhanjun Lu,^{1,5} and Wei Chen^{1,5,✉}

¹Ganzhou Key Laboratory of Greenhouse Vegetable, School of Life Sciences, Gannan Normal University, Ganzhou 341000, China, ²College of Plant Protection, Fujian Agriculture and Forestry University, Fuzhou 350002, China, ³South China Botanical Garden, Chinese Academy of Sciences, Guangzhou 510650, China, ⁴State Key Laboratory for Ecological Pest Control of Fujian and Taiwan Crops, Institute of Applied Ecology, Fujian Agriculture and Forestry University, Fuzhou 350002, China, and ⁵Corresponding author, e-mail: wy.he@fafu.edu.cn (W.H.), luzhanjun7@139.com (Z.L.), weichen@gnnu.edu.cn (W.C.)

*These authors contributed equally to this work.

Subject Editor: Konrad Fiedler

Received 16 September 2022; Editorial decision 8 November 2022.

Abstract

The glucosinolates (GLs) and myrosinase defensive systems in cruciferous plants were circumvented by *Plutella xylostella* using glucosinolate sulfatases (PxGSSs) during pest-plant interaction. Despite identifying three duplicated GSS-encoding genes in *P. xylostella*, limited information regarding their spatiotemporal and induced expression is available. Here, we investigated the tissue- and stage-specific expression and induction in response to GLs of PxGSS1 and PxGSS2 (PxGSS1/2) at the protein level, which shares a high degree of similarity in protein sequences. Western blotting (WB) analysis showed that PxGSS1/2 exhibited a higher protein level in mature larvae, their guts, and gut content. A significantly high protein and transcript levels of PxGSS1/2 were also detected in the salivary glands using WB and qRT-PCR. The immunofluorescence (IF) and immunohistochemistry (IHC) results confirmed that PxGSS1/2 is widely expressed in the larval body. The IHC was more appropriate than IF when autofluorescence interference was present in collected samples. Furthermore, the content of PxGSS1/2 did not change significantly under treatments of GL mixture from *Arabidopsis thaliana* ecotype Col-0, or commercial ally (sinigrin), 4-(methylsulfinyl)butyl, 3-(methylsulfinyl)propyl, and indol-3-ylmethyl GLs indicating that the major GLs from leaves of *A. thaliana* Col-0 failed to induce the expression of proteins for both PxGSS1 and PxGSS2. Our study systemically characterized the expression properties of PxGSS1/2 at the protein level, which improves our understanding of PxGSS1/2-center adaptation in *P. xylostella* during long-term insect-plant interaction.

Key words: diamondback moth, chewing-guild insect, counter-adaptation, spatiotemporal expression, insect-plant interaction

Plants update various constitutive and inducible defense mechanisms in response to biotic and abiotic factors (van Loon et al. 2006, Kessler 2015, Erb and Reymond 2019). In inducible defense, numerous secondary metabolites, such as alkaloid glucosides, benzoxazinoid glucosides, cyanogenic glucosides, iridoid glucosides, and salicinoids, enable host plants to rapidly defend themselves against insect attack (Zagrobelyny et al. 2004, Pentzold et al. 2014). These insect-plant interactions lead to the development of several arms races in which herbivores develop ingenious strategies to circumvent host plant defenses (Pentzold et al. 2014).

The interaction between a cruciferous specialist insect pest, *Plutella xylostella*, and its cruciferous hosts is classical and complex (Jander and Howe 2008, Winde and Wittstock 2011). Host

plants respond to pest attacks by activating a two-component defense system consisting of glucosinolates and myrosinases (Barth and Jander 2006, Bones and Rossiter 2010). Glucosinolates (GLs) are nitrogen- and sulfur-containing plant secondary metabolites. To date, 132 natural types of GLs have been identified. The biosynthesis of GLs and their metabolic pathway have been well documented. According to its basic structures, each unit consists of a β -thioglucose moiety, a sulfonated oxime moiety, and a variable side chain (also called R chain) (Halkier and Gershenzon 2006). Different types of GLs can be activated by corresponding myrosinases (or called β -thioglucosidases) that lead to a variety of toxic GLs-derived products, such as isothiocyanates (ITCs) and thiocyanates in cruciferous plants (Kliebenstein et al. 2005). Intriguingly, they function as

defensive factors exhibiting the antifeedant properties for herbivore larvae (Møldrup et al. 2012, Furlong et al. 2013) and oviposition stimuli for adult insects (Renwick et al. 2006, Liu et al. 2020).

Some insect herbivores can separately store GLs to tackle the challenge caused by the GLs-myrosinase system of plant. In addition, some evolve modified systems consisting of plants' GLs and insects' myrosinase (Winde and Wittstock 2011). Nevertheless, *P. xylostella* used an enzyme-based detoxification mechanism that did not result in the accumulation of toxic GLs-derived products in its larval body. For instance, *P. xylostella* use glucosinolate sulfatases (PxGSSs) to hydrolyze the sulfate group of glucosinolates to form the nontoxic GLs-derived products. The newly formed desulfo-GLs cannot be reacted further by plant myrosinase to generate poisonous ITCs (Ratzka et al. 2002). To date, three PxGSS genes that experienced twice duplication events have been identified, leading to an early differentiation of PxGSS3 and PxGSS1/2 (PxGSS1 or PxGSS2, hereafter named PxGSS1/2) and later differentiation of PxGSS1 and PxGSS2 (You et al. 2013, Heidel-Fischer et al. 2019). Based on a comparison of the coding sequences of PxGSS1, PxGSS2, and PxGSS3, PxGSS1 and PxGSS2 have a higher degree of similarity (Ma et al. 2018); however, all showed distinct substrate spectra based on *in vitro* enzyme activity tests (Heidel-Fischer et al. 2019). Moreover, *in vivo* functional study on PxGSSs, including RNAi-mediated knockdown and CRISPR/Cas9-based knockout experiments, revealed that PxGSS1 and PxGSS2 are the central counter-adaptation of *P. xylostella* against the plant GLs-myrosinase complex (Sun et al. 2019, Chen et al. 2020). The lack of knowledge about the refined protein expression pattern of PxGSS1/2 impacts our understanding of the role played by PxGSS1/2 in counter-adaptation to host plants. Besides, it remains unclear whether expressions of PxGSS1/2 are controlled or induced by the substrate of GLs. For instance, wild-type *Arabidopsis thaliana* (Col-0 ecotype) significantly upregulated the PxGSS1/2 transcript level compared with GLs-deficiency mutants, while no induced result of PxGSS1/2 was found at the protein level (Heidel-Fischer et al. 2019). Hence, it is imperative that further antibody-related studies are needed to fill the pending gaps comprehensively.

Several antibodies-based technologies were developed to explore the content and distribution of protein of interest, including Western blotting (WB), immunofluorescence (IF), and immunohistochemistry (IHC) (Renart et al. 1979, Towbin et al. 1979, Bekkouche et al. 2020). The success and repeatability of WB-based tests for protein content rely on several steps, including extracting proteins and determining signal normalization from different samples. Likewise, the IF and IHC techniques are the appropriate methods based on an image information-extracting system (Coons et al. 1941, Ramos-Vara 2005). The primary/secondary antibody is labeled with fluorescent dyes or a chromogenic reporter to visually examine specific protein characteristics under an electron microscope. Through the increasing use of WB, IF, and IHC, some important scientific issues in insects, such as insect development and metamorphosis, insect-microbe interactions, and insect chemoreception (Guo et al. 2018, Mancini et al. 2020, Tang et al. 2020, Zhang et al. 2022), have been well studied. However, no systematic comparison exists among different antibody-based detection systems for *P. xylostella*, resulting in no in-depth understanding of PxGSS1/2 protein distribution and expression, limiting our understanding of the *P. xylostella*-host interactions.

In this study, we investigated the protein expression properties of PxGSS1/2 in an economically important chewing-guild insect, *P. xylostella*. We developed PxGSS1/2 antibody-based detection systems for WB, IF, and IHC to investigate the expression pattern of PxGSS1/2 from different developmental stages and tissues in *P.*

xylostella. Moreover, to determine whether GLs induced PxGSS1/2, an artificial diet containing total GLs extract mixture or commercial (sinigrin), 4-(methylsulfinyl)butyl, 3-(methylsulfinyl)propyl, and indol-3-ylmethyl GLs were used respectively to feed larvae of *P. xylostella*, and the corresponding PxGSS1/2 content was determined. Our results provide significant insight into PxGSS1/2-centered interactions between specialist insects and host plants.

Materials and Methods

Insects and Plants Rearing

The *P. xylostella* strain was reared on an artificial diet without adding GL- or myrosinase-related ingredients (AD strain) (Huang et al. 2016). Insects were reared in an environment-controlled incubator. The uniform condition parameters were set as temperature at $25 \pm 1^\circ\text{C}$, light: dark cycle L:D = 16:8 hr, and relative humidity (RH) = $65 \pm 5\%$. *P. xylostella* adults were fed with 10 % honey water for oviposition. *A. thaliana* ecotype Columbia (Col-0) was grown in pots with mixed soil (perlite: vermiculite: humus = 1: 1: 1) in an environment-controlled chamber (ZRQ-250, Tuze, Shanghai, China) at a light: dark ratio of 16: 8, relative humidity of 60%, and a temperature of 22°C . Six-week-old *A. thaliana* leaves were used to extract total GLs.

Antibodies Preparations

To obtain the polyclonal antibody of PxGSS1/2, the homologous fragment 370–547 aa region in GSS1 (~20 kDa) was selected and combined with Glutathione S-transferase tag (GST) based on prokaryotic-based expression to generate the antigen (predicted molecular protein weight = 46 kDa). The PCR product was subcloned in pGEX-4T vector (preserved in our laboratory), and the recombinant plasmid of pGEX-4T-GSS1 was transferred into competent *Escherichia coli* Rosetta cells. When the OD value reaches 0.5–0.6 (wavelength = 600 nm), the component cells were induced by adding 0.8 mM isopropyl β -D-thiogalactoside (IPTG) at 37°C for four hours. The antigen affinity purification method was used for antibody purification, and the corresponding process was conducted in ABclonal Biotechnology Company (Wuhan, China). The house-keeping protein of monoclonal α -tubulin (1:5000, Sigma, T6074, USA) and the corresponding secondary antibodies of PxGSS1/2 (1:5000, Affinity, S0001, USA) or α -tubulin (1:10000, Sigma, A9044, USA) were purchased from corresponding companies.

Protein Extraction and WB

The four main methods of protein extraction, including phosphate buffer saline-disruption extraction (PBS-disruption extraction), radio immunoprecipitation assay solution-based extraction (RIPA extraction), phenol/sodium dodecyl sulfate-based extraction (phenol/SDS extraction), and Trizol-based protein extraction, were compared in this study. Besides, a commercial kit, named MinuteTM protein extraction kit (SD-001, Invent biotechnologies, Plymouth, MN), was used as a control. Finely ground larvae or different tissues were prepared under liquid nitrogen for PBS-disruption extraction and RIPA extraction (R0020, Solarbio, Beijing, China). The sample tubes were added with $100 \mu\text{l} \times \text{PBS}$ buffer (or RIPA lysis buffer for RIPA extraction). Following centrifuging at $12,000 \times g$ for 5 min, the supernatant was collected and ready for subsequent WB experiments. One milliliter Trizol reagent (Invitrogen, Carlsbad, CA) was added to the sample powder for Trizol-based protein extraction. Instead of RNA extraction, we washed the protein precipitate with 1 ml of 95% ethanol containing 0.3 mol/liter guanidine hydrochloride. Protein was

dissolved in 1% SDS solution, and the insoluble matter was removed by centrifugation at $10,000 \times g$ for 10 min at 4°C . For phenol/SDS extraction, 0.8 ml phenol and 0.8 ml dense SDS buffer (30% sucrose, 2% SDS, 0.1 M Tris-HCl, pH 8.0, 5% 2-mercaptoethanol) were added into sample powder. The supernatant was transferred to a new centrifuge tube following centrifugation at $10,000 \times g$ for 3 min. A five-time volume of methanol was added into the tube and thoroughly mixed upside down. After freezing at -20°C for one hour, the precipitate was obtained by centrifuging at $10,000 \times g$ for five minutes, followed by two washes with 80% cold acetone. After air-drying for 5–10 min, the precipitate was diluted with 1% SDS, and the soluble part was used for WB. The 10 μg of total protein from samples collected from different developmental stages or tissues in 3rd-instar larvae ($n = 3$) were loaded onto the gel, and WB was performed as described previously (Chen et al. 2020).

Spatiotemporal Sample Collections

We measured the distribution patterns of PxGSS1/2 in different developmental stages and tissues. We collected ~150 eggs, 10 1st-instar larvae, three 2nd-, 3rd-, and 4th-instar larvae, three pupae, and three female and male adults. For tissue collections, the dissection sequence is as follows: 15 4th-instar larvae sterilized with 75% alcohol were individually transferred onto a new Petri dish containing 1 \times PBS buffer. The heads of larvae were dissected to obtain the paired salivary glands (Sag) and silk glands (Sg); subsequently, the whole gut and Malpighian tubules (Mt) were sampled from the dissected body. In addition, the whole gut was dissected to collect the contents in the gut (gut contents, Gc), and the gut was separated into three parts, including foreguts (Fg), midguts (Mg), and hindguts (Hg). The rest parts were washed with 1 \times PBS buffer three times to pool into a new 1.5 ml centrifuge tube to obtain samples of the residual body (Rb). Three biological repeats were conducted.

Total RNA Extraction and qRT-PCR of PxGSS1 and PxGSS2

The dissected tissue samples were collected in three biological replicates for the quantitative real-time PCR (qRT-PCR) experiments. Trizol reagent (5301100, Simgen, Hangzhou, China) and first strand cDNA synthesis kit (7306100, Simgen, Hangzhou, China) were used for RNA extraction and cDNA preparation, respectively. qRT-PCR was conducted using Hieff UNICON qPCR SYBR Green Master Mix (YEASEN, 11199ES03, China) in LightCycle96 PCR Detection System (Roche, Basel, Switzerland) and corresponding primer information was referred to Chen et al. (2020) listed in Supp Table 1 (online only). All operations were performed according to the manufacturer's instructions.

Immunofluorescence and Immunohistochemistry

The dehydrator and embedding machines (JT-12J and JB-L5, Junjie Electronics Co., Ltd., Huizhou, Guangdong, China) were used for paraffin embedding of 4th-instar larval samples, and the slicer (RM2016, Leica, Wetzlar, Germany) was used for paraffin slides prepared for the staining of hematoxylin/eosin (HE). As part of the dewaxing operation, paraffin sections were placed in xylene twice for 15 min, anhydrous ethanol for 5 min, and subsequently treated with 85 and 75% alcohol for five minutes before being washed with distilled water. For IF experiments, sections were transferred to the EDTA buffer and placed in a microwave oven box (pH = 8.0). After the sections were treated with fluorescence quenching inhibitor (S2110, Solarbio, Beijing, China) and blocked with 1% BSA for 30 min, they were incubated for two hours with primary antibody of

PxGSS1/2 (1:200, diluted in TBST) and TRITC-labelled secondary antibody (T-2769, Thermo). The sections ($n = 3$) were washed three times with 1 \times TBST between two antibody incubations, and finally, a drop of blocking solution with nuclear acid dye (DAPI) was applied before the sections were sealed by epoxy. The IF experiments of salivary glands without cross section were repeated according to the process described earlier in this paper ($n = 3$). The sample without primary antibody of PxGSS1/2 was used for the control.

For the IHC experiment, the dewaxing sections ($n = 3$) were placed into citrate buffer antigen retrieval (pH = 6.0, C1032, Solarbio, Beijing, China). A solution of 3% H_2O_2 was used to block endogenous peroxidase activity. The corresponding sections were blocked with rabbit serum (SL034, Solarbio, Beijing, China) for 30 min before incubation with the PxGSS1/2 (1:200, diluted in PBS) and HRP-labelled secondary antibody (1: 500, diluted in PBS, SE134, Solarbio, Beijing, China). The final images were observed using a slide scanning system (Pannoramic MIDI, 3D Histech Ltd., Budapest, Hungary) under a DAB kit (DA1010, Solarbio, Beijing, China) and counterstaining with hematoxylin.

Extraction and Content Determination of Total GLs

Total intact GLs were extracted from the leaves powder (0.3 g) of *A. thaliana* Col-0 using an extraction solution, including 1 ml boiled 70% methanol (enzymes inactivation) and 10 μl of the internal standard of 10 mM sinigrin (85440, Sigma-Aldrich, St. Louis, MO). The homogeneous mixture was incubated for 15 min. in water at 75°C . After centrifuging at 12,000 rpm (13,523 rcf) for 5 min, the supernatant was dried on a rotatory evaporator to remove the solvent. It was re-suspended in 1 ml distilled water followed by filtration with a 0.22- μm filter membrane.

To quantify the GLs content in sampled leaves of *A. thaliana* Col-0, the supernatant was transferred to a purification column containing a syringe where the bottom was covered with cotton, and the body was filled with DEAE Sephadex A25 (A25120, Sigma-Aldrich) pre-treated by 2 mol/liter acetic acid solution and 6 mol/liter imidazole formate. Subsequently, the purification column was incubated with sulfatase solution (10 μM , S9626, Sigma-Aldrich) overnight at room temperature and was eluted with 200 μl distilled water. The 10 μl of corresponding elution was loaded onto a high-performance liquid chromatography column (column: SB-C18, HPLC: Agilent 1260, Santa Clara, CA). The parameters of HPLC (UV = 229 nm) and response factors relative to the internal standard sinigrin were described in the previous article (Grosser and van Dam 2017).

GLs-Containing Feeding Assays

We applied a 200 μl mixture of total GLs (850 μM) and allyl GL (sinigrin), 4-(methylsulfinyl)butyl, 3-(methylsulfinyl)propyl, and indol-3-ylmethyl (20 μM) solutions to the surface of artificial diet slices ($25 \times 23 \times 2$ mm). The sinigrin was purchased from Sigma-Aldrich company (85440, $\geq 99\%$, USA) and 4-(methylsulfinyl)butyl, 3-(methylsulfinyl)propyl, and indol-3-ylmethyl were from Huaster biology company (HB-07722, HB-00019, and HB-07717, $\geq 98\%$, Huhang, China). The 3rd-instar larvae were transferred onto the artificial diet for 12- and 24-hr feeding. The AD strain larvae feeding the original artificial diet for 0, 12, and 24 hr were used for control and named CK-0hr, CK-12hr, and CK-24hr, respectively. Furthermore, for the treatment group, the larvae feeding on total GLs (or other four different GL solutions) at the 12- or 24-hr postingestion were collected and labeled as T-12hr and T-24hr, where T denoted for other four different GL treatments and detailed information was marked

in the figure legend. Each group contained three bioreplicates, and each one contained three larvae. Total proteins were extracted from collected samples using phenol/SDS method and subjected to WB experiments.

Statistical Analysis

The gray values of protein bands in WB figure were transformed using Image J (version 1.51). The relative protein expression was calculated by comparing the gray value of PxGSS1/2 with α -tubulin. The Shapiro-Wilk test for normality and Levene's test for homogeneity of variances were used for statistical analysis (GraphPad Prism; version 8.4.3). One-way ANOVA method (or Brown-Forsythe ANOVA if heterogeneity in variances) followed by a Tukey's HSD post hoc test (or Games-Howell's multiple comparisons) was used for the significant difference analysis of data ($P < 0.05$). Figures were drawn by GraphPad Prism (version 8.4.3).

Results

Phenol/SDS-Based Protein Extraction Method is Compatible With WB Assays

The total protein abundance was first compared using four different protein extraction methods, including PBS-disruption extraction, RIPA extraction, phenol/SDS extraction, and Trizol-based protein extraction. Besides, a commercial kit equipped with the grinding pestle was also used for control (Supp Fig. 1 [online only]). Based on electrophoresis results of equal amounts of protein samples (20 μ g) from the 3rd- or 4th-instar larvae, the phenol/SDS extraction method resulted in high protein abundance from high to low molecular weight, which is nearly consistent with the Trizol-based protein method and commercial kit (Supp Fig. 1 [online only]). To determine the compatibility of different methods for further WB, samples of 3rd- or 4th-instar larvae were collected, and the monoclonal antibody of α -tubulin was used for further testing. In the phenol/SDS and Trizol-based protein methods, the protein was detected with a clear band of the expected molecular weight of α -tubulin. However, no signals of α -tubulin were detected in PBS-disruption and RIPA extraction of two larval-stage samples (Supp Fig. 2A and B [online only]). Subsequently, the phenol/SDS method was used to extract the protein from different tissues of the 4th-instar larvae. There was no significant difference found in the signal of α -tubulin among residual body, salivary glands, Malpighian tubules, and midguts ($F_{3,8} = 1.91$, $P = 0.2071$) (Supp Fig. 2C [online only]).

Antibody Preparation and Specificity Test of PxGSS1/2

PxGSS1 and PxGSS2 have identical lengths and a high level of similarity (~95%). Therefore, the predicted molecular weight of the protein is the same as ~61 kDa. By comparing the amino acid differences in conserved domains between PxGSS1 and PxGSS2, we found that the signal peptide domain (SP), N-acetylgalactosamine 4-sulfatase (NA4S), and unknown domain (UD) of two proteins contained 2, 10 and 11 different amino acids. To obtain the antibody of these two proteins, the homologous fragment of PxGSS1 and PxGSS2 (~20 kDa; 93%) was selected for antibody preparation (AP) of PxGSS1/2 (Fig. 1A). The antigen was expressed in a prokaryotic expression system with GST tag (~26 kDa) and induced by different concentrations of IPTG in the form of an inclusion body (Supp Fig. 3A [online only]). The result of protein purification showed that PxGSS1/2 protein was successfully recovered (Supp Fig. 3B [online only]). Based on the WB, less than 500 pg of antigen was detected by the polyclonal antibody of PxGSS1/2 and the molecular weight is

46 kDa (Fig. 1B). To further analyze the specificity of the polyclonal antibody of PxGSS1/2 in endogenous conditions, the total protein of 3rd-instar larvae or corresponding midguts was extracted by the phenol/SDS method. Based on the WB, the single band (>60 kDa) found in both samples indicated that the polyclonal antibody of PxGSS1/2 is compatible with the exploration of the fine expression pattern of PxGSS1/2 protein (Fig. 1C).

Developmental- and Tissue-Specific Distribution Patterns of GSS1/2

To measure the relative protein level of PxGSS1/2, the gray value of PxGSS1/2 was divided by the value of α -tubulin in different samples. PxGSS1/2 exhibited a high expression pattern among all developmental stages except for two, adults and eggs. The expression of PxGSS1/2 was relatively high in 3rd- and 4th-instar larvae; however, there was no significant difference between these two stages ($F_{6,4} = 10.58$, $P = 0.0152$) (Fig. 2A and B). To further explore the detailed distribution pattern of PxGSS1/2 in larvae, 4th-instar larvae were used to dissect related tissues. The total content of PxGSS1/2 in the salivary glands and guts expressed high compared to the silk glands and Malpighian tubules ($F_{7,5} = 12.63$, $P = 0.0054$) (Fig. 2C and D). Although no α -tubulin was detected in the gut content, the gut content showed a relatively high content of PxGSS1/2 when the gray value of PxGSS1/2 was divided by the highest value of α -tubulin in the silk gland (Fig. 2C and D). Likewise, at the transcript level, the *PxGSS1* gene was highly expressed in the salivary glands and foregut ($F_{6,14} = 19.42$, $P < 0.0001$), meanwhile *PxGSS2* gene was highly expressed in foregut ($F_{6,14} = 16.54$, $P < 0.0001$). However, both genes exhibited relatively low expression in Malpighian tubules and were rarely expressed in silk glands (Fig. 3).

Immunochemical Distribution Analyses of PxGSS1/2

The paraffin section from the 4th-instar larvae was stained with hematoxylin and eosin to identify the nucleus and cytoplasm, respectively (Fig. 4A). The clear distinction between gut content and peritrophic membrane was found in the longitudinal section (Fig. 4B and C). Paraffin sections were further incubated with the antibody of PxGSS1/2 to perform IF. The sections incubated with secondary antibodies and without secondary antibodies were used as experimental and control groups, respectively. The autofluorescence was found in control (Fig. 4D); however, the experimental group detected the stronger red fluorescent signals in the cuticle and peritrophic membrane of the midgut (Fig. 4E). To determine whether salivary glands contained PxGSS1/2, salivary glands were dissected for direct IF experiments. The significantly stronger fluorescence signal of PxGSS1/2 was found in PxGSS1/2 antibody-incubated group as compared to the control (Fig. 5).

To overcome autofluorescence, the IHC method was used to test the distribution of PxGSS1/2. PxGSS1/2 was not detected in the control group of paraffin sections incubated only with secondary antibodies (Fig. 6A). Nevertheless, there was a detection of a clear and comprehensive distribution in cuticle, and gut content in the section treated with the polyclonal antibody of PxGSS1/2 and a secondary antibody (Fig. 6B). PxGSS1/2 was detected in the gut (fore, mid, and hindgut), gut content, and outer regions, including muscles and hemocytes (Fig. 6C).

GL-Response Characteristic of PxGSS1/2 at Protein Level

To reveal whether substrate GL induced PxGSS1/2, the total GLs extracted from the leaves of *A. thaliana* Col-0 were applied to the surface of the artificial diet slice (25 \times 23 \times 2 mm). The level

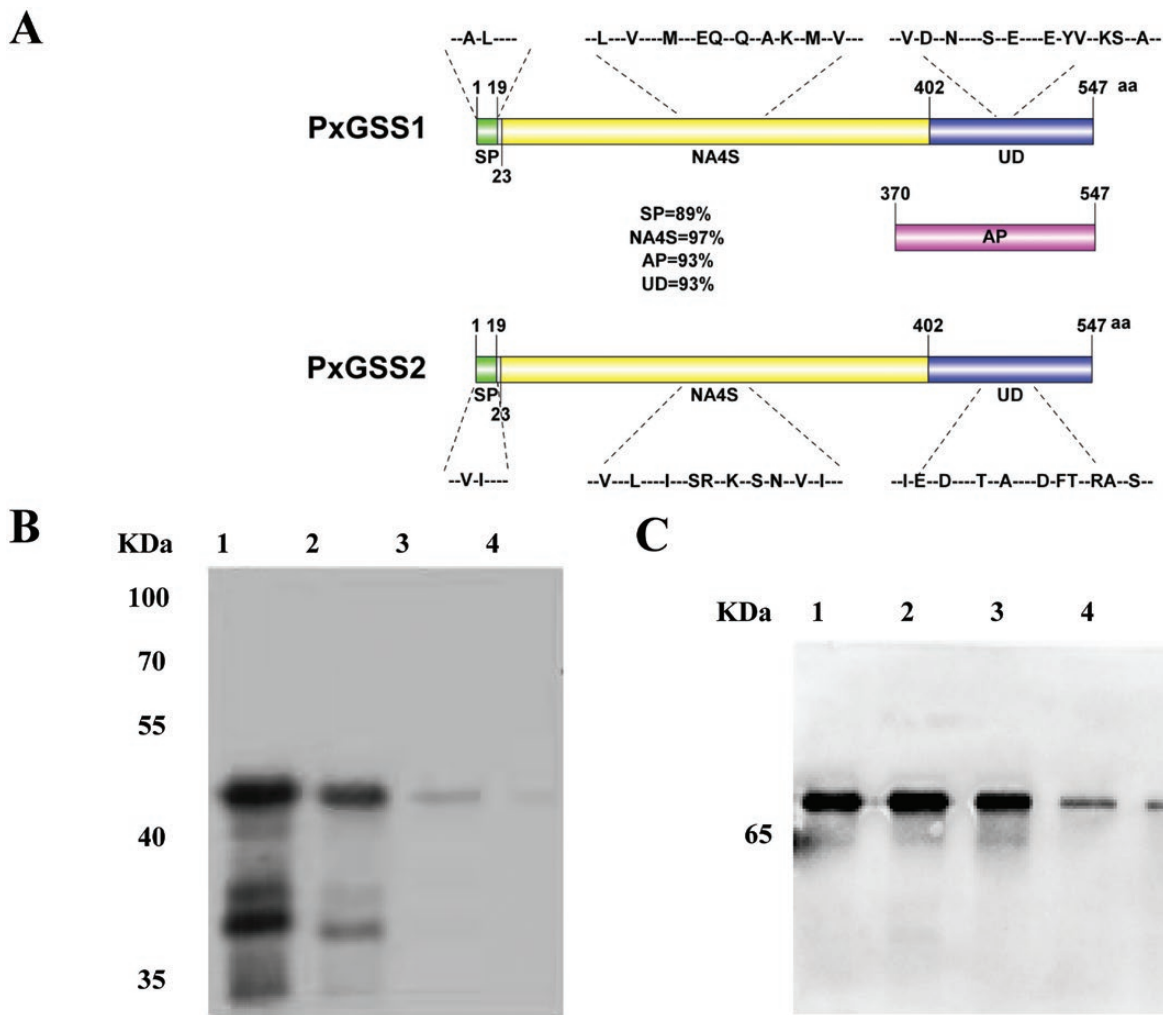


Fig. 1. Protein structural analysis and antibody specificity for PxGSS1/2. (A) Protein sequence comparison between PxGSS1 and PxGSS2 based on deduced amino acid sequences. SP: signal peptide; NA4S: N-acetylgalactosamine 4-sulfatase domain; UD: unknown domain; AP: antigen protein. The same amino acids were indicated in the short dash, and the differences were presented in the standard single-letter abbreviation. (B) The *in vitro* test of PxGSS1/2 antibody-based on WB result. Lane 1–4: 10 ng, 5 ng, 1 ng, and 500 pg of antigen protein were used in WB. (C): The *in vivo* test of PxGSS1/2 antibody-based on WB result. Each three biological protein samples were extracted from the 3rd-instar larvae (Lane 1–3) and the corresponding midguts (Lane 4–6). The phenol/SDS extraction method was used in protein extraction.

of PxGSS1/2 protein did not significantly differ between samples collected 12- and 24-hr post-treatment ($F_{4,10} = 2.938$, $P = 0.0760$) (Fig. 7A). Moreover, the commercial substances of sinigrin (the substrate of PxGSS1, not PxGSS2), 4-(methylsulfinyl)butyl, 3-(methylsulfinyl)propyl, and indol-3-ylmethyl GLs were used to test the inducibility of PxGSS1 and PxGSS2. Likewise, no significant difference was found in the content of PxGSS1/2 protein among the samples from 12- and 24- hours after each treatment, including sinigrin ($F_{4,10} = 1.088$, $P = 0.4132$), 4-(methylsulfinyl)butyl GL ($F_{4,10} = 1.211$, $P = 0.3650$), 3-(methylsulfinyl)propyl GL ($F_{4,10} = 0.9162$, $P = 0.4913$), and indol-3-ylmethyl GL ($F_{4,10} = 0.4129$, $P = 0.7957$) (Fig. 7B–E).

Discussion

In this study, we firstly compared the applications of four different protein extraction methods using WB and found that phenol/SDS was compatible with WB-based quantification. We used the detection system of WB for a comprehensive investigation of the distribution

of PxGSS1/2 protein *in vivo*. The larvae, their gut, and gut contents contain a high expression of PxGSS1/2, which is consistent with the previous report (Ratzka et al. 2002). Intriguingly, a significantly high level of PxGSS1/2 was also detected in salivary glands at both transcript and translation levels. Furthermore, our IF and IHC results also confirmed that PxGSS1/2 is widely expressed. Notably, the protein levels of PxGSS1/2 did not change significantly upon exposure to total GLs or commercial sinigrin, 4-(methylsulfinyl)butyl, 3-(methylsulfinyl)propyl, and indol-3-ylmethyl GLs, suggesting that the expressions of PxGSS1 and PxGSS2 are independent of major GLs in *A. thaliana* Col-0.

To date, three known PxGSSs have undergone two rounds of differentiation. PxGSS1 and PxGSS2 are young paired duplicated genes distributed in tandem with PxGSS3 in the genome of *P. xylostella* (You et al. 2013, Heidel-Fischer et al. 2019). The sulfatase C is the common ancestor gene of these three genes, and PxGSS1/2 is the close ancestor gene of both PxGSS1 and PxGSS2 (Heidel-Fischer et al. 2019). It has been demonstrated that a single undifferentiated gene, PxGSS1/2, is still present in the *Plutella australiana*, which

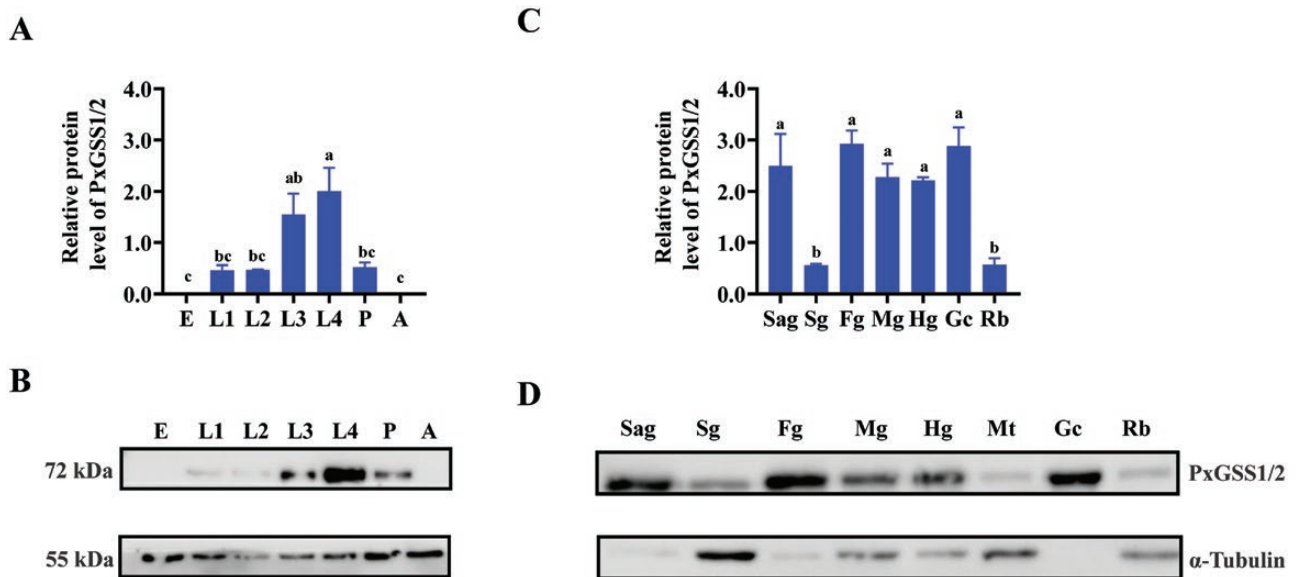


Fig. 2. Developmental- and tissue-specific protein expression of PxGSS1/2. (A) The relative protein level and (B) one representative WB result of PxGSS1/2 in the different developmental stages. The relative protein level (C) and one representative WB result of PxGSS1/2 (D) in different tissues. Acronyms used on X-axis: E: eggs; L1–4: From 1st- to 4th-instar larvae; P: pupae; A: adults; Sag: salivary glands; Sg: silk glands; Fg: foreguts; Mg: midguts; Hg: hindguts; Mt: Malpighian tubules; Gc: gut contents; Rb: residual body. Results are shown as means \pm S.E. ($n = 3$). Lowercase letters denote significant differences among the samples ($P < 0.05$). The α -tubulin of Sg was used as an internal reference for Gc.

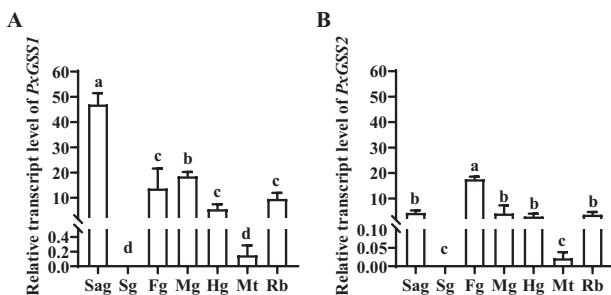


Fig. 3. Tissue-specific relative transcript levels of PxGSS1 and PxGSS2 gene using qRT-PCR. The gene relative transcript level of PxGSS1 (A) and PxGSS2 (B) in the different tissues dissected from 4th-instar larvae. The abbreviations of different tissues are the same as in Fig. 2. Results are shown as means \pm S.E. ($n = 3$). Lowercase letters denote significant differences among the samples ($P < 0.05$).

is a relative species of *P. xylostella* (Landry and Paul 2013, Perry et al. 2018). Consequently, it is impossible to generate individual antibodies due to the high similarity and the same length of each protein. Despite being a polyclonal antibody, a clear single band of ~72 kDa was detected in different samples, suggesting that PxGSS1 and PxGSS2 are superimposed. This result is consistent with the previous antibody results obtained with different PxGSS1/2 mutants (Chen et al. 2020), indicating that this epitope is suitable for developing specific antibodies. Based on WB results of PxGSS1/2 among two PxGSS1 and one PxGSS1 mutant lines, the content of PxGSS1 was about twice that of PxGSS2 (Chen et al. 2020). Currently, the known protein modifications on PxGSS include glycosylation and formylation (Ratzka et al. 2002, Heidel-Fischer et al. 2019). The glycosylation of proteins contributes to internal folding, proteostasis, functional stability, and transportation of proteins. This process occurs primarily in the endoplasmic reticulum (ER) (Varki 2016, Schjoldager et al. 2020). In the adult mosquito, *Aedes aegypti*, an approximately 7-kDa molecular weight difference

was found between glycosylated and de-glycosylated leucine-rich repeat-containing G protein-coupled receptor 1 (Rocco et al. 2017). Glycosylated and deglycosylated PxGSS1/2 showed similar weight changes (Heidel-Fischer et al. 2019). The formylation, produced by sulfatases modification factor SUMF1a and 1b, is present in all the sulfatases to enable PxGSSs biological activity (Ratzka et al. 2002). However, the single amino acid change (transformation from cysteine to formylated-glycine) has little effect on the molecular weight of protein. The band specificity of our results suggests that the polyclonal antibody of PxGSS1/2 is suitable and robust for subsequent immunofluorescence and immunohistochemical studies.

Immunofluorescence has been widely used in the study of *P. xylostella* in many aspects, including reproductive regulation, embryonic development, interactions between host and pathogen, and resistance to *Bacillus thuringiensis* toxins (Kwon and Kim 2008, Guo et al. 2020, Peng et al. 2020, Zou et al. 2020, Li et al. 2021). Nevertheless, autofluorescence is a common problem in IF, and minimizing it becomes important in ensuring the accuracy of results (Beutner et al. 1965, Tang et al. 2020). The observation of *P. xylostella* slices showed that IHC is more effective than IF in avoiding the interference of endogenous signals. In this study, we found that the control group for IHC was free of interference from spurious signals. Indeed, the IHC technology has been successfully applied to *P. xylostella* (Escrive et al. 1995, Zhang et al. 2020). Hence, considering immunochemical data are qualitative and the existence of autofluorescence in *P. xylostella*, therefore, multiple methods should be combined to investigate the distribution pattern of protein of interest thoroughly.

Our results demonstrated that the protein expression pattern of PxGSS1/2 exhibited relatively high in mature larvae and low at other developmental stages. These results are consistent with the gene expressions of PxGSS1 and PxGSS2 (Ratzka et al. 2002, Ma et al. 2018). However, little is known about the mechanism of transcription and translation of PxGSS1 and PxGSS2. Larvae are exposed to long-term stimulation of glucosinolates and other secondary metabolites. Therefore, we speculated that these substances

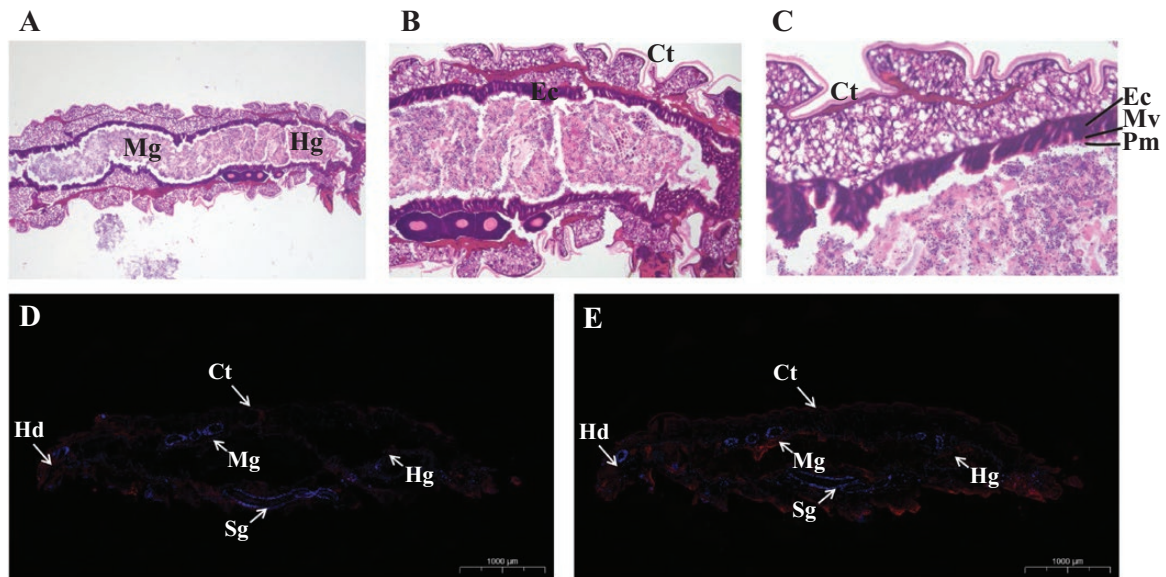


Fig. 4. Immunofluorescence of PxGSS1/2 based on larval paraffin section. The hematoxylin and eosin (HE) staining of the paraffin section was dissected from 4th-instar larvae in (A) 40x, (B) 100x, and (C) 200x magnification. The blue color represents the nucleus, and the red is the cytoplasm. Immunofluorescence results of paraffin section dissected from 4th-instar larvae. (D) and (E): Middle-layer paraffin sections, pre-incubated with the polyclonal antibody of PxGSS1/2, were untreated or treated with fluorescent-labeled secondary antibody, respectively. (Scale bar: 1,000 μm). Abbreviations used in the figure: Mg: midgut; Hg: hindgut; Ct: cuticle; Ec: enterocytes; Mv: microvilli; Pm: peritrophic membrane; Hd: Head; Sg: silk gland. Blue fluorescent signals: DAPI; red fluorescent signals: PxGSS1/2 protein.

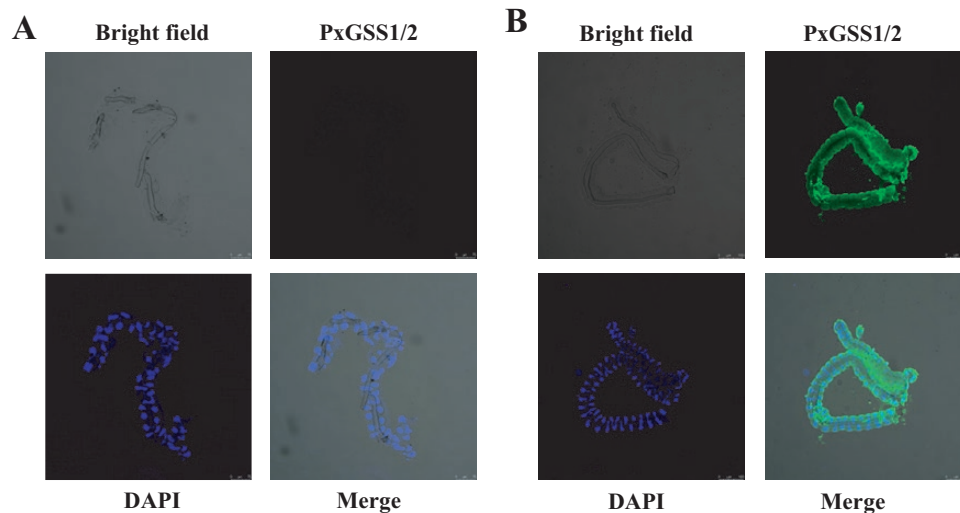


Fig. 5. Immunofluorescence of PxGSS1/2 based on salivary glands. The salivary glands incubated without (A) or with (B) primary antibody of PxGSS1/2. Blue fluorescent signals: DAPI; green fluorescent signals: PxGSS1/2 protein. Scale bar: 100 μm .

could potentially regulate the expression of mRNA and protein of PxGSS1 and PxGSS2. In adults, *P. xylostella* depends on GLs-derived products, such as the volatile gas of isothiocyanate (ITC), for host finding. Among 12 female-biased expressed olfactory receptors (Or), proteins Or35 and Or49 responded specifically to three ITC compounds of iberberin, 4-pentenyl ITC, and phenylethyl ITC, revealing the molecular mechanism underlying female adult preference for oviposition (Liu et al. 2020).

Furthermore, GLs and GLs-derived products play a significant role in the insect-plant relationship and tritrophic interactions. Sun et al. (2019) reported that *A. thaliana*-mediated RNAi significantly reduced PxGSS1 gene expression and enzyme activity, leading to suppression of larval growth and survival due to an accumulation

of ITCs (Sun et al. 2019). Therefore, it remains unclear which substance, such as GL, GL-derived products, or others, regulates the expression of PxGSS1 and PxGSS2 at the mRNA level, which should be further investigated.

A higher level of PxGSS1/2 was detected in the whole gut (fore, mid, and hindgut). Our findings are similar to the previous study where PxGSS1/2 found higher levels in the intact gut and gut contents (Ratzka et al. 2002). In addition, we also detected a significantly higher concentration of PxGSS1/2 in salivary glands using WB and qRT-PCR. The numerous effectors and elicitors in saliva from various insects have been extensively documented (Mutti et al. 2008, Erb and Reymond 2019, Xu et al. 2019). Recent reports have suggested that PxGSS1 can be released onto attacked plant leaves

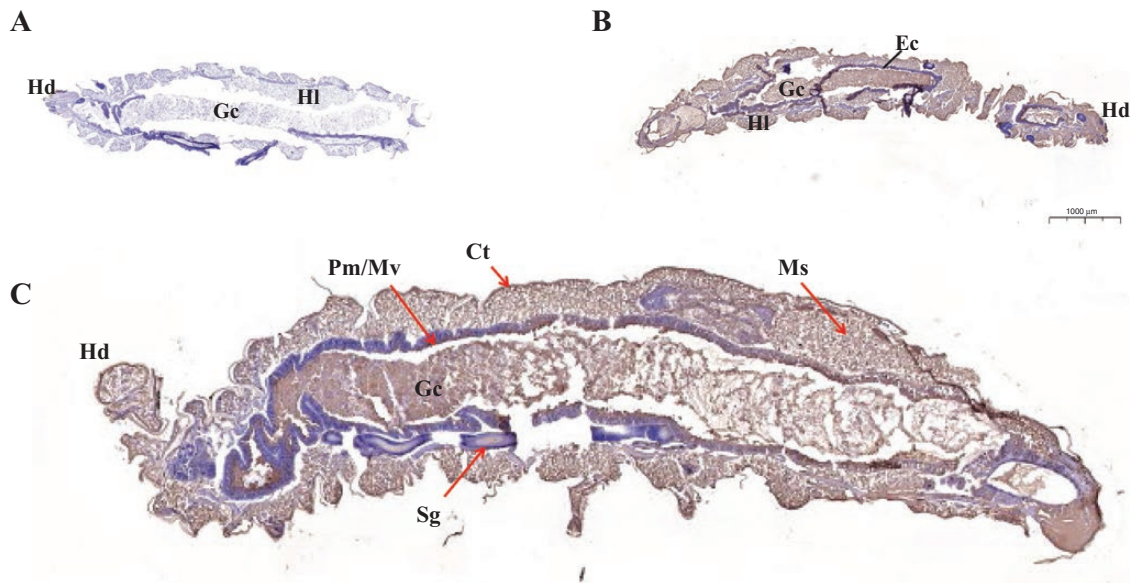


Fig. 6. Immunohistochemistry of PxGSS1/2 based on larval paraffin section. (A) Paraffin sections were directly incubated with HRP-labelled secondary antibody. (B) and (C) Paraffin sections were incubated with the polyclonal antibody of PxGSS1/2, followed by the HRP-labelled secondary antibody. Brown signal: PxGSS1/2 protein stained by DAB method; blue signal: nuclei stained by hematoxylin. Abbreviations used in the figure; Hd: head; HI: hemolymph; Gc: gut content; Ec: enterocytes; Pm/Mv: peritrophic membrane/microvilli; Ct: cuticle; Sg: silk gland; Ms: muscle. (Scale bar: 1,000 µm).

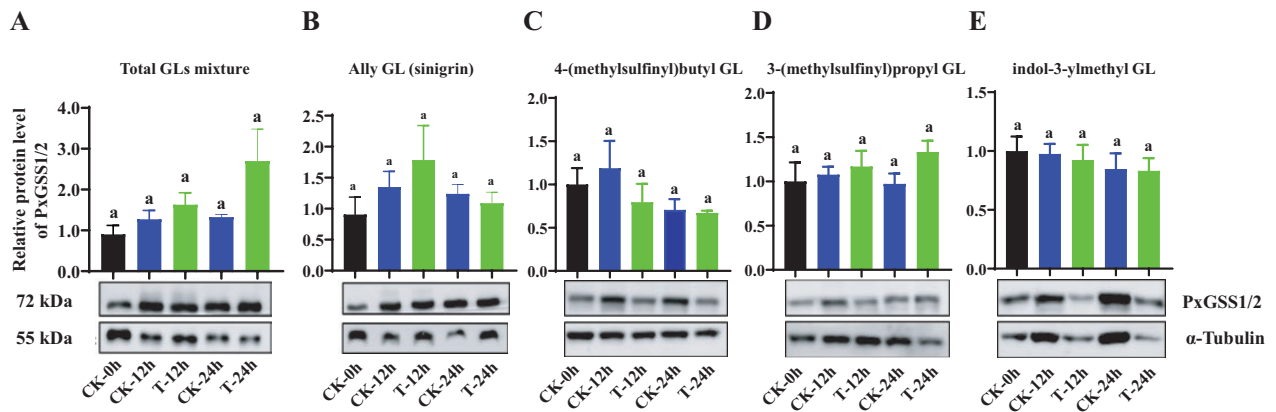


Fig. 7. The detection of relative PxGSS1/2 expression feeding on a GL-containing diet. The WB results and PxGSS1/2 expression from 3rd-instar larvae were fed on a total GLs-adding diet (A) or sinigrin (B), 4-(methylsulfinyl)butyl (C), 3-(methylsulfinyl)propyl (D), and indol-3-ylmethyl GLs (E) -adding diet at different times. Acronyms used on X-axis: CK: larvae feeding on GL-free diet; T: larvae feeding on the diet slices treated by total GL mixture (850 µM, 200 µl), or commercial substances of sinigrin, 4-(methylsulfinyl)butyl, 3-(methylsulfinyl)propyl, and indol-3-ylmethyl GLs (20 µM, 200 µl). The three-time points are 0, 12, and 24 hr. The relative protein expression of PxGSS1/2 was calculated by comparing the gray value of PxGSS1/2 to that of α -tubulin. Each treatment contained three biological replicates, and each covered three intact larvae.

to pre-detoxify defensive GLs of the host plant (Chen et al. 2022). Therefore, salivary glands may be the source of the released PxGSS1. In order to detect whether PxGSS1 and PxGSS2 are constitutive or inducible proteins, total GLs were extracted from *A. thaliana* and applied to an artificial diet to feed 3rd-instar larvae after starvation of four hours. Our study found that the protein content of PxGSS1 and PxGSS2 did not differ significantly between the treatment and control groups in two time points. Further, we repeated the above experiments using a single GL, sinigrin (a substrate for PxGSS1 but not for PxGSS2), and three other high-content GLs in *A. thaliana* Col-0, including 4-(methylsulfinyl)butyl, 3-(methylsulfinyl)propyl, and indol-3-ylmethyl GLs. These three GLs accounted for 53.6, 6.9, and 9.1% of the total GLs content in the Col-0 ecotype (Hanschen et al. 2018), respectively. We found that PxGSS1/2 signals were not upregulated after GLs treatment compared with the

control group. In a nutshell, we speculated that the major substrate GLs from *A. thaliana* Col-0 could induce neither PxGSS1 nor PxGSS2. Previously, it was found that translation and transcription of PxGSS1/2 are asynchronous in *P. xylostella* larvae fed wild-type and GL-deficient mutant *A. thaliana* Col-0 plants (Heidel-Fischer et al. 2019). Accordingly, there is a possible explanation for this non-conformity. Some specific GLs may induce the mRNA level, but a series of regulation mechanisms at the post-transcriptional level will restrict the over-translation of the protein PxGSS1 and PxGSS2. The over-expression of PxGSS1/2 becomes a burden for *P. xylostella*, which needs to balance energy distribution for defense and growth. However, this assumption needs to be investigated.

In *A. thaliana*, the content of total GLs varied with the genotype, developmental stage, tissues, and growing conditions. However, the average range is approximately 70 µmol/g (4-(methylsulfinyl)butyl,

4-(methylsulfanyl)butyl, and indol-3-ylmethyl GL) in fresh weight in Col-0 type, which accounting for >70 % of total GLs content (Hanschen et al. 2018). Indeed, ten mM GLs or 3.5 mM indol-3-ylmethyl GL were added to the diet for feeding experiments with *Bemisia tabaci* (Malka et al. 2016). Due to the higher concentration of GLs extracted in our study than that in *A. thaliana* and other GL-containing feeding experiments, we conclude that the protein expressions of PxGSS1 and PxGSS2 are not influenced by GL concentration, and both are GL-independently expressed. Similarly, the GSS was highly expressed in the *B. tabaci* whether rearing on GL-rich or GL-free diets (Manivannan et al. 2021). Interestingly, another member of PxGSS3 was induced by Trp-GL at both mRNA and protein levels in *P. xylostella* (Heidel-Fischer et al. 2019). Likewise, the enzymatic activity of GSS showed a 10-fold change when the polyphagous locust *Schistocerca gregaria* consumed GL-rich or GS-low host plants (Falk and Gershenzon 2007). A constitutive (PxGSS1/2)-inducible (PxGSS3) enzymatic model at the protein level may exist in *P. xylostella*, enabling it to metabolize various glucosinolates for rapid detoxification. However, the enzyme activities of three PxGSSs were conferred by SUMF1a and 1b through post-translational modification (Chen et al. 2022). Therefore, the inducible effect of GLs on GSSs should require full consideration of SUMF1a and 1b during insect-plant interaction. Given this complexity, the inducibilities of three GSSs at the enzyme activity level need to be further investigated in the future.

In summary, PxGSS1/2 is widely expressed in different larval tissues, including the digestive and salivary secretion systems. Further, the major GLs from leaves of *A. thaliana* Col-0 failed to induce the expression of proteins for both constitutive PxGSS1 and PxGSS2 enzymes, which play an important role in counter-adaptation to the host plant by disarming the GL-myrosinase defense. The full-armed characteristics of *P. xylostella* allow it to specialize in cruciferous plants broadening our understanding of insect-plant interactions. Therefore, we conclude that PxGSS1/2 is the control target, and the PxGSS-related inhibitors need urgently be developed for application in pest control of *P. xylostella*.

Acknowledgments

We are grateful to Y.J. Wen of South China Agricultural University for assisting in glucosinolate extractions and quantitative analyses. We are also grateful to H.Z. Yu and X.D. Yu of Gannan Normal University for partial discussions in manuscript and data performance. The work was supported by a grant from National Natural Science Foundation of China (32260721), the Science and Technology Foundation of Education Department of Jiangxi Province for Young Scholar (GJJ201450), College Students' Innovation and Entrepreneurship Training Program of GanNan Normal University (CX210066), and Talent Program of Jiangxi (jxsq2020102133).

Author Contributions

Conceptualization, WH, ZL, and WC; methodology in antibody, YX and CJ; software, MBA, YD, and LX; insect rearing, YX, LX, and YL; sample collection, YX, YL; original draft preparation, WC and MBA; review and editing, WC, MBA, WH, and ZL; supervision, WH, ZL, and WC; funding acquisition, ZL and WC; All authors have read and agreed to the published version of the manuscript.

Supplementary Data

Supplementary data are available at *Journal of Insect Science* online.

References Cited

- Barth, C., and G. Jander. 2006. *Arabidopsis* myrosinases TGG1 and TGG2 have redundant function in glucosinolate breakdown and insect defense. *Plant J.* 46: 549–562.
- Bekkouche, B., H. K. Fritz, E. Rigosi, and D. C. O'carroll. 2020. Comparison of transparency and shrinkage during clearing of insect brains using media with tunable refractive index. *Front. Neuroanat.* 14: 599282.
- Beutner, E. H., E. J. Holborow, and G. D. Johnson. 1965. A new fluorescent antibody method: mixed antiglobulin immunofluorescence or labelled antigen indirect immunofluorescence staining. *Nature.* 208: 353–355.
- Bones, A. M., and J. T. Rossiter. 2010. The myrosinase-glucosinolate system, its organisation and biochemistry. *Physiol. Plantarum.* 97: 194–208.
- Chen, W., Y. H. Dong, H. S. A. Saqib, L. Vasseur, W. W. Zhou, L. Zheng, Y. F. Lai, X. L. Ma, L. Y. Lin, X. J. Xu, et al. 2020. Functions of duplicated glucosinolate sulfatases in the development and host adaptation of *Plutella xylostella*. *Insect Biochem. Mol. Biol.* 119: 103316.
- Chen, W., H. S. A. Saqib, X. Xu, Y. Dong, L. Zheng, Y. Lai, X. Jing, Z. Lu, L. Sun, M. You, et al. 2022. Glucosinolate sulfatases–sulfatase-modifying factors system enables a crucifer-specialized moth to pre-detoxify defensive glucosinolate of the host plant. *J. Agric. Food Chem.* 70: 11179–11191.
- Coons, A. H., H. J. Creech, and R. N. Jones. 1941. Immunological properties of an antibody containing a fluorescent group. *Proc. Soc. Exp. Biol. Med.* 47: 200–202.
- Erb, M., and P. Reymond. 2019. Molecular interactions between plants and insect herbivores. *Annu. Rev. Plant Biol.* 70: 527–557.
- Escrive, B., B. Tabashnik, N. Finson, and J. Ferre. 1995. Immunohistochemical detection of binding of Cry1a crystal proteins of *Bacillus thuringiensis* in highly resistant strains of *Plutella xylostella* (L.) from Hawaii. *Biochem. Biophys. Res. Commun.* 212: 388–395.
- Falk, K. L., and J. Gershenzon. 2007. The desert locust, *Schistocerca gregaria*, detoxifies the glucosinolates of *Schouwia purpurea* by desulfation. *J. Chem. Ecol.* 33: 1542–1555.
- Furlong, M. J., D. J. Wright, and L. M. Dossall. 2013. Diamondback moth ecology and management: problems, progress, and prospects. *Annu. Rev. Entomol.* 58: 517–541.
- Grosser, K., and N. M. Van Dam. 2017. A straightforward method for glucosinolate extraction and analysis with high-pressure liquid chromatography (HPLC). *J. Vis. Exp.* 121: e55425.
- Guo, S. Y., W. M. Wu, S. Y. Li, Y. Liu, Z. Ruan, M. Q. Ye, Y. Xiao, Y. J. Zhong, Y. Cao, and K. Li. 2018. 20-Hydroxyecdysone-upregulated proteases involved in *Bombyx* larval fat body destruction. *Insect. Mol. Biol.* 27: 724–738.
- Guo, Z., S. Kang, D. Sun, L. Gong, J. Zhou, J. Qin, L. Guo, L. Zhu, Y. Bai, F. Ye, et al. 2020. MAPK-dependent hormonal signaling plasticity contributes to overcoming *Bacillus thuringiensis* toxin action in an insect host. *Nat. Commun.* 11: 3003.
- Halkier, B. A., and J. Gershenzon. 2006. Biology and biochemistry of glucosinolates. *Annu. Rev. Plant Biol.* 57: 303–333.
- Hanschen, F. S., M. Pfitzmann, K. Witzel, H. Stutzel, M. Schreiner, and R. Zrenner. 2018. Differences in the enzymatic hydrolysis of glucosinolates increase the defense metabolite diversity in 19 *Arabidopsis thaliana* accessions. *Plant Physiol. Biochem.* 124: 126–135.
- Heidel-Fischer, H. M., R. Kirsch, M. Reichelt, S. J. Ahn, N. Wielsch, S. W. Baxter, D. G. Heckel, H. Vogel, and J. Kroymann. 2019. An insect counteradaptation against host plant defenses evolved through concerted neofunctionalization. *Mol. Biol. Evol.* 36: 930–941.
- Huang, Y., Y. Chen, B. Zeng, Y. Wang, A. A. James, G. M. Gurr, G. Yang, X. Lin, Y. Huang, and M. You. 2016. CRISPR/Cas9 mediated knockout of the abdominal-A homeotic gene in the global pest, diamondback moth (*Plutella xylostella*). *Insect Biochem. Mol. Biol.* 75: 98–106.
- Jander, G., and G. Howe. 2008. Plant interactions with arthropod herbivores: state of the field. *Plant Physiol.* 146: 801–803.
- Kessler, A. 2015. The information landscape of plant constitutive and induced secondary metabolite production. *Curr. Opin. Insect Sci.* 8: 47–53.
- Kliebenstein, D. J., J. Kroymann, and T. Mitchell-Olds. 2005. The glucosinolate–myrosinase system in an ecological and evolutionary context. *Curr. Opin. Plant Biol.* 8: 264–271.

- Kwon, B., and Y. Kim. 2008. Transient expression of an EP1-like gene encoded in *Cotesia plutellae* bracovirus suppresses the hemocyte population in the diamondback moth, *Plutella xylostella*. *Dev. Comp. Immunol.* 32: 932–942.
- Landry, J. F., and H. Paul. 2013. *Plutella australiana* (Lepidoptera, Plutellidae), an overlooked diamondback moth revealed by DNA barcodes. *Zookeys*. 327: 43–63.
- Li, T. P., L. W. Zhang, Y. Q. Li, M. S. You, and Q. Zhao. 2021. Functional analysis of the orphan genes Tssor-3 and Tssor-4 in male *Plutella xylostella*. *J. Integr. Agric.* 20: 1880–1888.
- Liu, X. L., J. Zhang, Q. Yan, C. L. Miao, W. K. Han, W. Hou, K. Yang, B. S. Hansson, Y. C. Peng, J. M. Guo, et al. 2020. The molecular basis of host selection in a crucifer-specialized moth. *Curr. Biol.* 30: 4476–4482.e5.
- Ma, X. L., W. Y. He, W. Chen, X. J. Xu, W. P. Qi, M. M. Zou, Y. C. You, S. W. Baxter, P. Wang, and M. S. You. 2018. Structure and expression of sulfatase and sulfatase modifying factor genes in the diamondback moth, *Plutella xylostella*. *Insect Sci.* 25: 946–958.
- Malka, O., A. Shekhov, M. Reichelt, J. Gershenzon, D. G. Vassão, and S. Morin. 2016. Glucosinolate desulfation by the phloem-feeding insect *Bemisia tabaci*. *J. Chem. Ecol.* 42: 230–235.
- Mancini, M. V., C. Damiani, S. M. Short, A. Cappelli, U. Ulissi, A. Capone, A. Serrao, P. Rossi, A. Amici, C. Kalogris, et al. 2020. Inhibition of *Asaia* in adult mosquitoes causes male-specific mortality and diverse transcriptome changes. *Pathogens*. 9: 380.
- Manivannan, A., B. Israni, K. Luck, M. Gotz, E. Seibel, M. Easson, R. Kirsch, M. Reichelt, B. Stein, S. Winter, et al. 2021. Identification of a sulfatase that detoxifies glucosinolates in the phloem-feeding insect *Bemisia tabaci* and prefers indolic glucosinolates. *Front. Plant Sci.* 12: 671286.
- Møldrup, M. E., F. Geu-Flores, M. De Vos, C. E. Olsen, J. Sun, G. Jander, and B. A. Halkier. 2012. Engineering of benzylglucosinolate in tobacco provides proof-of-concept for dead-end trap crops genetically modified to attract *Plutella xylostella* (diamondback moth). *Plant Biotechnol. J.* 10: 435–442.
- Mutti, N. S., J. Louis, L. K. Pappan, K. Pappan, K. Begum, M. S. Chen, Y. Park, N. Dittmer, J. Marshall, J. C. Reese, et al. 2008. A protein from the salivary glands of the pea aphid, *Acyrtosiphon pisum*, is essential in feeding on a host plant. *Proc. Natl. Acad. Sci. U. S. A.* 105: 9965–9969.
- Peng, L., Q. Wang, M. M. Zou, Y. D. Qin, L. Vasseur, L. N. Chu, Y. L. Zhai, S. J. Dong, L. L. Liu, W. Y. He, et al. 2020. CRISPR/Cas9-mediated vitellogenin receptor knockout leads to functional deficiency in the reproductive development of *Plutella xylostella*. *Front. Physiol.* 10: 1585.
- Pentzold, S., M. Zagrobelny, F. Rook, and S. Bak. 2014. How insects overcome two-component plant chemical defence: plant β -glucosidases as the main target for herbivore adaptation. *Biol. Rev.* 89: 531–551.
- Perry, K. D., G. J. Baker, K. J. Powis, J. K. Kent, C. M. Ward, and S. W. Baxter. 2018. Cryptic *Plutella* species show deep divergence despite the capacity to hybridize. *BMC Evol. Biol.* 18: 1–17.
- Ramos-Vara, J. 2005. Technical aspects of immunohistochemistry. *Vet. Pathol.* 42: 405–426.
- Ratzka, A., H. Vogel, D. J. Kliebenstein, T. Mitchell-Olds, and J. Kroymann. 2002. Disarming the mustard oil bomb. *Proc. Natl. Acad. Sci. U. S. A.* 99: 11223–11228.
- Renart, J., J. Reiser, and G. R. Stark. 1979. Transfer of proteins from gels to diazobenzoyloxymethyl-paper and detection with antisera: a method for studying antibody specificity and antigen structure. *Proc. Natl. Acad. Sci. U. S. A.* 76: 3116–3120.
- Renwick, J. A., M. Haribal, S. Gouinguéné, and E. Städler. 2006. Isothiocyanates stimulating oviposition by the diamondback moth, *Plutella xylostella*. *J. Chem. Ecol.* 32: 755–766.
- Rocco, D. A., D. H. Kim, and J. V. Paluzzi. 2017. Immunohistochemical mapping and transcript expression of the GPA2/GPB5 receptor in tissues of the adult mosquito, *Aedes aegypti*. *Cell Tissue Res.* 369: 313–330.
- Schjoldager, K. T., Y. Narimatsu, H. J. Joshi, and H. Clausen. 2020. Global view of human protein glycosylation pathways and functions. *Nat. Rev. Mol. Cell Biol.* 21: 729–749.
- Sun, R., X. Jiang, M. Reichelt, J. Gershenzon, S. S. Pandit, and D. Giddings Vassão. 2019. Tritrophic metabolism of plant chemical defenses and its effects on herbivore and predator performance. *eLife*. 8: e51029.
- Tang, X. T., F. Ibanez, and C. Tamborindeguy. 2020. Quenching autofluorescence in the alimentary canal tissues of *Bactericera cockerelli* (Hemiptera: Trioziidae) for immunofluorescence labeling. *Insect Sci.* 27: 475–486.
- Towbin, H., T. Staehelin, and J. Gordon. 1979. Electrophoretic transfer of proteins from polyacrylamide gels to nitrocellulose sheets: Procedure and some applications. *Proc. Natl. Acad. Sci. U. S. A.* 76: 4350–4354.
- Van Loon, L. C., M. Rep, and C. M. Pieterse. 2006. Significance of inducible defense-related proteins in infected plants. *Annu. Rev. Phytopathol.* 44: 135–162.
- Varki, A. 2016. Biological roles of glycans. *Glycobiology*. 27: 3–49.
- Winde, I., and U. Wittstock. 2011. Insect herbivore counteradaptations to the plant glucosinolate-myrosinase system. *Phytochemistry*. 72: 1566–1575.
- Xu, H. X., L. X. Qian, X. W. Wang, R. X. Shao, Y. Hong, S. S. Liu, and X. W. Wang. 2019. A salivary effector enables whitefly to feed on host plants by eliciting salicylic acid-signaling pathway. *Proc. Natl. Acad. Sci. U. S. A.* 116: 490–495.
- You, M., Z. Yue, W. He, X. Yang, G. Yang, M. Xie, D. Zhan, S. W. Baxter, L. Vasseur, G. M. Gurr, et al. 2013. A heterozygous moth genome provides insights into herbivory and detoxification. *Nat. Genet.* 45: 220–225.
- Zagrobelny, M., S. Bak, C. T. Ekström, C. E. Olsen, and B. L. Møller. 2004. Cyanogenic glucosides and plant–insect interactions. *Phytochemistry*. 65: 293–306.
- Zhang, Z., J. Kong, S. D. Mandal, S. Li, Z. Zheng, F. Jin, and X. Xu. 2020. An immune-responsive PGRP-S1 regulates the expression of antibacterial peptide genes in diamondback moth, *Plutella xylostella* (L.). *Int. J. Biol. Macromol.* 142: 114–124.
- Zhang, Q., Z. Li, D. Chen, S. Wu, H. Wang, Y. Li, and Z. Lei. 2022. The molecular identification, odor binding characterization, and immunolocalization of odorant-binding proteins in *Liriomyza trifolii*. *Pestic. Biochem. Physiol.* 181: 105016.
- Zou, M. M., Q. Wang, L. N. Chu, L. Vasseur, Y. L. Zhai, Y. D. Qin, W. Y. He, G. Yang, Y. Y. Zhou, and L. Peng, et al. 2020. CRISPR/Cas9-induced vitellogenin knockout lead to incomplete embryonic development in *Plutella xylostella*. *Insect Biochem. Mol. Biol.* 123: 103406.